Glycerol dialkyl glycerol tetraethers in surficial coastal and open marine sediments around China: Indicators of sea surface temperature and effects of their sources

CrossMark

Haoda Zhou [a,b,e], Jianfang Hu [a,*], Baruch Spiro [a,c], Ping'an Peng [a], Jianhui Tang [d]

[a] State Key Laboratory of Organic Geochemistry, Guangzhou Institute of Geochemistry, Chinese Academy of Sciences, Guangzhou, 510640, PR China
[b] Graduate University of Chinese Academy of Sciences, Beijing, 100049, PR China
[c] Department of Mineralogy, The Natural History Museum, Cromwell Road, London SW7 5BD, UK
[d] Yantai Institute of Coastal Zone Research for Sustainable Development, Chinese Academy of Sciences, Yantai, 264003, PR China
[e] Zhuhai Central Station of Marine Environmental Monitoring, State Oceanic Administration, Zhuhai 519015, China

ARTICLE INFO

ABSTRACT

Accurate reconstruction of past sea surface temperature (SST) is important for the understanding of past climate and its variations. Recently, the TEX_{86} indicator (TetraEther indeX of tetraethers consisting of 86 carbon atoms), based on glycerol dialkyl glycerol tetraethers (GDGTs) has been developed into a promising proxy for SST reconstruction. In this study, we investigated the distribution of GDGTs in surficial sea bottom sediments from coastal and open marine settings around China between 18°N and 38°N in water depth of either <100 or >1000 m. As the distribution patterns of GDGTs reflect their biological sources and their respective habitats these can be identified from the sediment samples investigated. The distributions of branched GDGTs (brGDGTs) in the Yellow Sea (YS) was found to be similar to that of the lower Yellow River basin indicating that the brGDGTs in the YS originated from terrestrial soil. While the variability of the cyclisation ratio of branched tetraethers (CBT)-derived pH values in the Pearl River estuary (PRE) suggested that brGDGTs might also be produced in situ in coastal sediments or in the water column. In the shallow areas (water depth <100 m, the YS, East China Sea and PRE) TEX_{86}^H-based SST (SST_{86}^H) was overestimated or underestimated when compared with mean annual $SST_{satellite}$, most likely caused by seasonality or overprint by a cold-biased terrestrial signal. In the South China Sea (SCS), at water depth >1000 m, the SST_{86}^H matched well the mean annual SST determined by satellite, indicating the applicability of the TEX_{86}^H temperatures for paleoclimate investigations in these study areas and, potentially, in similar settings of deep water. These findings provide the basis for application of branched/isoprenoid index (BIT) and TEX_{86} as indicators for temperature and paleotemperature in coastal and open marine environments around China.

© 2013 Elsevier B.V. All rights reserved.

1. Introduction

Accurate reconstruction of sea surface temperature (SST) is important for understanding past climate and its variation. Therefore, large efforts have been made to determine the variations in SST throughout the geological history (IPCC, 2007) using indicators such as $\delta^{18}O$ and Mg/Ca ratios of planktonic foraminifera and indicative lipids. Lipid-based proxy indicators for SST include U_{37}^K-indices, a ratio index of long-chain unsaturated alkenone (Brassell et al., 1986), and TEX_{86} proxy and its derivatives, based on glycerol dialkyl glycerol tetraethers (GDGTs) from Archaea (e.g. Schouten et al., 2002; Kim et al., 2008, 2010).

GDGTs are membrane lipids of Archaea and bacteria (Sinninghe Damsté et al., 2000; Weijers et al., 2006a) and exist in both isoprenoid and branched forms, derived from different sources, which are still being investigated. Isoprenoid GDGTs (isoGDGTs) are produced by at least two groups of Archaea, Thaumarchaeota (formerly marine group I Crenarchaeota) and Euryarchaeota, and usually have acyclic or ring-containing biphytanyl chains (De Rosa and Gambacorta, 1988; Brochier-Armanet et al., 2008; Spang et al., 2010, and references therein). One isoGDGT, thaumarchaeol (formerly crenarchaeol), and its regio-isomer, have been postulated to be specific to Thaumarchaeota (Brochier-Armanet et al., 2008) and was originally considered to be synthesized only by nonthermophilic marine members of this phylum (Sinninghe Damsté et al., 2002). However, it was subsequently detected in a culture of thermophilic nitrifying Thaumarchaeota (De La Torre et al., 2008), in microbial mats in terrigenous geothermal hot springs (Pearson et al., 2004; Zhang et al., 2006; Schouten et al., 2007) and in soils adjacent to terrigenous geothermal hot springs (Pitcher et al., 2009). The TEX_{86} proxy was proposed by Schouten et al. (2002), for the estimation of past SST by quantifying the average number of cyclopentane rings in tetraethers with 86 carbon atoms in sediments. It appears not to be dependent on salinity or nutrient concentration (Wuchter et al., 2004, 2005). The proxy TEX_{86} has been successfully

applied to the calculation of paleotemperature histories of aquatic systems in sediments from oceans and large lakes (e.g. Powers et al., 2004, 2010). Kim et al. (2010) modified the TEX_{86}-SST calibration model by distinguishing TEX_{86}^H-SST and TEX_{86}^L-SST calibration models for SST above 15 °C (H) and SST below 15 °C (L), respectively.

Branched GDGTs (brGDGTs) are generally attributed to soil bacteria (Sinninghe Damsté et al., 2000; Weijers et al., 2006b) possibly Acidobacteria (Sinninghe Damsté et al., 2011). A GDGT proxy, the BIT (branched/isoprenoid) index, was proposed and applied to determine the relative inputs of soil organic matter (OM) to aquatic environments (Hopmans and Weijers, 2004; Walsh et al., 2008). The cyclisation ratio of branched tetraethers (CBT), based on the structures of brGDGTs varying in the amount of cyclopentane moieties, was found to correlate with measured soil pH (Weijers et al., 2007). However, recent studies suggest that brGDGTs have diverse origins. For example, brGDGTs can be the result of in situ production in lacustrine sediments (e.g. Tierney et al., 2010) in addition to the soil bacterial source. Schouten et al. (2007) found brGDGTs also in sediments and microbial mats in hot springs. Hu et al. (2012) detected brGDGTs in pelagic sediments in locations where the contribution from soils can be discounted. These findings indicate that brGDGTs can be produced not only in soils but also in aquatic environments.

In recent years, the distribution of GDGT-proxies has been increasingly used in studies of China's marginal seas. Several studies investigated the distributions of GDGTs in the sediments and water in the South China Sea (SCS) (e.g. Wei et al., 2011; Jia et al., 2012), and discovered that TEX_{86}-based SSTs temperatures were overall lower than the measured surface water temperatures. It seems therefore that TEX_{86} reflects a deeper and cooler subsurface temperature in the SCS (Jia et al., 2012). Thus, it is proposed that the temperature difference between the U_{37}^K and TEX_{86} reflects changes of depth of the mixed layer in the SCS (Jia et al., 2012; Li et al., 2013). Moreover, Ge et al. (2013) and Zhang et al. (2013) showed that TEX_{86}-derived temperatures were lower than the mean annual SSTs in the inner shelf areas of the SCS, and deduced that the TEX_{86}-derived temperatures mainly reflected the winter SSTs in the coastal region of the SCS. However, Shintani et al. (2011) found that the TEX_{86} temperature corresponds to the SSTs in warmer seasons in the open northern SCS. While for the East China Sea, TEX_{86}-derived temperature is robust and reflects the annual mean SST (Zhu et al., 2011). These recent studies show the need and importance of constraining the GDGT-proxies on regional scales for temperature reconstruction. Therefore, a systematic study of the distribution of GDGTs and their application as temperature proxies in the seas around China is necessary.

In this study, we investigated the distribution of GDGTs in surface sediments from coastal and open marine settings around China between 18°N and 38°N in water depth of either <100 or >1000 m. The main goals of this study of surface sediments taken along transects in various oceanographic settings of coastal and open marine sediments around China were: 1) to determine the distribution of GDGTs, 2) to determine the relative contribution of their marine and terrestrial sources, 3) to derive temperature estimates, 4) to explore the potential of the observations and results to decipher other processes and effects. This study tests the TEX_{86}^H, as temperature indicator in comparison with SST determined from satellites, and BIT indicator as relative input of terrestrial and marine GDGTs. This study should provide a reference for future investigations of records of paleoclimate in sediments from the seas around China using these proxies.

2. Materials and methods

2.1. Sites and sample collection

The study of the sea off the coast of China was carried out on samples from the following areas 1) the Yellow Sea (YS), 2) the East China Sea (ECS), and 3) the adjacent South China Sea (SCS), which includes the Pearl River estuary (PRE) (Fig. 1). The respective SST data of each station were retrieved from NODC (Levitus) World Ocean Atlas 1994
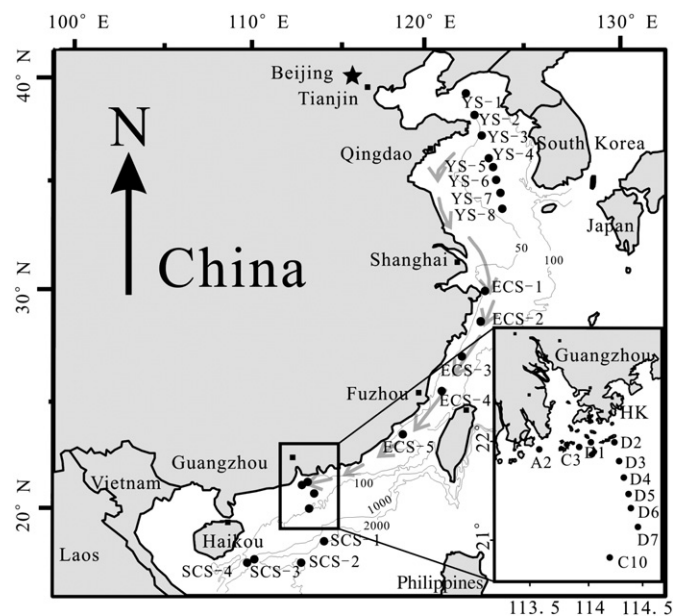

Fig. 1. Map of the study area showing sample locations indicated by circles (●).

(NODC_WOA94) from the Web site of http://www.esrl.noaa.gov/psd/on a 1° grid resolution and monthly long term mean parameters by satellite remote sensing. We used average values of the annual mean climatology SST data to explore the relationships of the distribution of isoprenoid GDGTs (calculated as TEX_{86}^H) with SST measured from satellites, for the four seasons as follows: spring, March–May; summer, June–August; autumn, September–November; winter, December–February.

The YS is a semi-enclosed shallow basin (mean water depth 44 m) with relatively low water exchange with the open ocean. The waters are strongly influenced by the YS coastal water and the YS warm current. The weather in this region is characterized by cold and dry winters and warm and wet summers, with an annual mean SST of 16 °C. The water in the ECS is influenced by China's coastal current and Taiwan's warm current and has a mean SST of 22 °C. The SCS is one of the largest marginal seas in the Western Pacific, with an annual mean SST of 23 °C in the northern coastal area. The Pearl River system discharges into the SCS via three sub-estuaries: the Lingdingyang, Modaomen, and Huangmaohai estuaries. The coastal waters in the estuary are strongly influenced by three water regimes: Pearl River discharge, oceanic water from the SCS, and coastal water from the South China coastal current (Ying, 1994).

Surface sediment samples were collected with a stainless steel grab sampler from the coastal and open marine areas around China. Seventeen samples were collected in September 2006 in the YS, ECS, SCS, and ten samples were collected in July 2002 in the Pearl River estuary. All sediment samples were stored at -18 °C until analysis.

2.2. Extraction and analytical procedures

Sediment samples were freeze dried and homogenized in preparation for lipid extraction by Soxhlet reflux for 48 h using a mixture of dichloromethane (DCM) and methanol (2:1, V/V). The resulting mixture was centrifuged and the organic phase was separated from the aqueous phase using a separation funnel after addition of 5% KCl solution. The aqueous layer was extracted with DCM (×2). The collected organic phase was concentrated by rotary evaporation. The total lipid extract was fractionated into apolar and polar fractions using a column packed with activated alumina using hexane/DCM (9:1, V/V) and DCM/methanol (1:1, V/V) as eluents, respectively.

The polar fraction was dried under a stream of N_2, redissolved in hexane/propanol (99:1, V/V) and filtered through a 0.45 μm polytetrafluoroethylene (PTFE) filter. Lipid analysis was performed

Table 1

Concentrations of glycerol dialkyl glycerol tetraethers (GDGTs) present in surface sediments, the branched vs. isoprenoid tetraether index (BIT), the cyclisation ratio of branched tetraethers (CBT)-derived pH, the tetraether index of tetraethers consisting of 86 carbon atoms (TEX$_{86}^{H}$)-derived SST (SST$_{86}^{H}$) and satellite-derived seasonal temperatures (spring, summer, autumn and winter).

| Sample	Latitude (°N)	Longitude (°E)	Depth (m)	IsoGDGTs (ng g^{-1} dw)	BrGDGTs (ng g^{-1} dw)	GDGT-0 (ng g^{-1} dw)	Thaumarchaeol (ng g^{-1} dw)	BIT	CBT-pH	TEX$_{86}^{H}$	SST$_{86}^{H}$ (°C)	Spring	Summer	Autumn	Winter	SST$_{satellite}$
YS-1	38.76′N	122.73′E	53.7	253.9	50.1	91.2	102.7	0.19	9.0	−0.33	16.0	7.9	21.1	18.7	6.1	13.4
YS-2	37.76′N	123.02′E	61.6	136.5	38.7	51.6	53.6	0.28	8.5	−0.34	15.3	8.0	21.1	18.8	6.7	13.6
YS-3	36.77′N	123.30′E	69.7	73.2	40.9	23.9	30.4	0.42	8.4	−0.29	18.8	8.5	21.4	19.3	7.6	14.2
YS-4	35.73′N	123.58′E	84.5	416.6	122.2	150.1	167.7	0.23	9.2	−0.31	17.4	9.1	21.8	19.8	8.5	14.8
YS-5	35.25′N	123.73′E	77.0	271.1	57.1	90.8	113.3	0.17	9.1	−0.31	17.4	9.1	21.8	19.8	8.5	14.8
YS-6	34.77′N	123.84′E	79.6	150.6	40.6	51.4	61.6	0.25	8.6	−0.33	16.0	10.0	22.3	20.3	9.6	15.6
YS-7	34.18′N	124.00′E	80.4	274.7	35.7	87.6	113.3	0.13	8.7	−0.32	16.7	10.6	22.1	20.3	10.2	15.8
YS-8	33.42′N	124.01′E	64.6	216.5	31.1	60.4	92.1	0.16	8.3	−0.28	19.4	11.8	22.8	21.1	11.6	16.8
Mean				**224.1**	**52.1**	**75.9**	**91.8**	**0.23**	**8.7**	**−0.31**	**17.1**	**9.4**	**21.8**	**19.7**	**8.6**	**14.9**
ECS-1	30.15′N	123.20′E	60.2	234.0	22.6	51.4	102.2	0.10	8.4	−0.21	24.2	14.8	25.0	23.1	14.5	19.3
ECS-2	28.64′N	122.39′E	53.6	463.1	83.9	80.0	212.6	0.19	8.0	−0.23	22.9	17.7	26.5	24.3	16.9	21.3
ECS-3	27.23′N	121.38′E	49.3	370.5	62.2	58.2	181.0	0.17	7.9	−0.21	24.2	21.7	27.0	24.7	17.9	22.2
ECS-4	25.83′N	120.40′E	58.4	470.5	60.0	86.7	219.9	0.14	7.8	−0.25	21.5	21.7	27.5	25.4	19.6	23.5
ECS-5	24.13′N	118.46′E	42.2	78.1	17.4	12.8	38.4	0.21	8.0	−0.26	20.8	22.6	27.5	25.6	20.3	24.0
Mean				**323.2**	**49.2**	**57.8**	**150.8**	**0.16**	**8.0**	**−0.23**	**22.7**	**19.2**	**26.7**	**24.6**	**17.8**	**22.1**
SCS-1	19.25′N	114.80′E	1363	368.8	23.3	66.3	157.5	0.09	7.8	−0.17	27.0	25.9	28.9	27.2	23.6	26.4
SCS-2	18.23′N	113.68′E	1302	457.9	34.7	87.87	178.77	0.11	8.1	−0.18	26.3	26.3	29.0	27.4	24.1	26.7
SCS-3	18.28′N	111.55′E	1288	415.5	29.9	69.4	178.7	0.10	7.8	−0.16	27.7	26.0	29.0	27.3	23.9	26.6
SCS-4	18.08′N	110.69′E	1207	426.0	58.3	59.9	199.6	0.15	7.8	−0.22	23.6	25.9	29.0	27.3	23.8	26.5
Mean				**417.1**	**36.6**	**70.9**	**178.6**	**0.11**	**7.8**	**−0.18**	**26.2**	**26.0**	**29.0**	**27.3**	**23.8**	**26.5**
A2	21.95′N	113.45′E	9	139.7	185.7	26.0	63.0	0.68	7.4	−0.25	21.5	–	–	–	–	–
C3	21.96′N	113.88′E	25	302.4	84.1	58.2	145.1	0.28	7.4	−0.26	20.8	24.4	28.3	26.4	22.1	25.3
C10	20.83′N	114.13′E	85	192.4	32.3	27.0	94.2	0.17	8.0	−0.20	24.9	25.3	28.7	26.9	22.9	25.9
D1	22.01′N	114.03′E	16	433.9	144.7	77.8	201.1	0.34	7.2	−0.28	19.4	24.6	28.4	26.5	22.2	25.5
D2	21.97′N	114.27′E	29	263.6	91.5	61.4	113.5	0.36	7.4	−0.23	22.9	24.6	28.4	26.5	22.2	25.5
D3	21.80′N	114.30′E	39	168.6	64.7	36.1	71.8	0.37	7.5	−0.27	20.1	24.6	28.4	26.5	22.2	25.5
D4	21.62′N	114.33′E	46	163.0	55.6	30.2	73.4	0.33	7.6	−0.25	21.5	24.6	28.4	26.5	22.2	25.5
D5	21.45′N	114.37′E	59	270.9	77.3	44.9	127.3	0.28	7.7	−0.22	23.6	24.6	28.4	26.5	22.2	25.5
D6	21.30′N	114.40′E	67	133.8	43.6	22.6	60.4	0.31	7.8	−0.22	23.6	24.6	28.4	26.5	22.2	25.5
D7	21.12′N	114.45′E	79	95.9	25.9	17.3	42.8	0.27	7.9	−0.21	24.2	24.6	28.4	26.5	22.2	25.5
Mean				**216.4**	**80.5**	**40.2**	**99.3**	**0.34**	**7.6**	**−0.24**	**22.2**	**24.7**	**28.5**	**26.6**	**22.4**	**25.6**
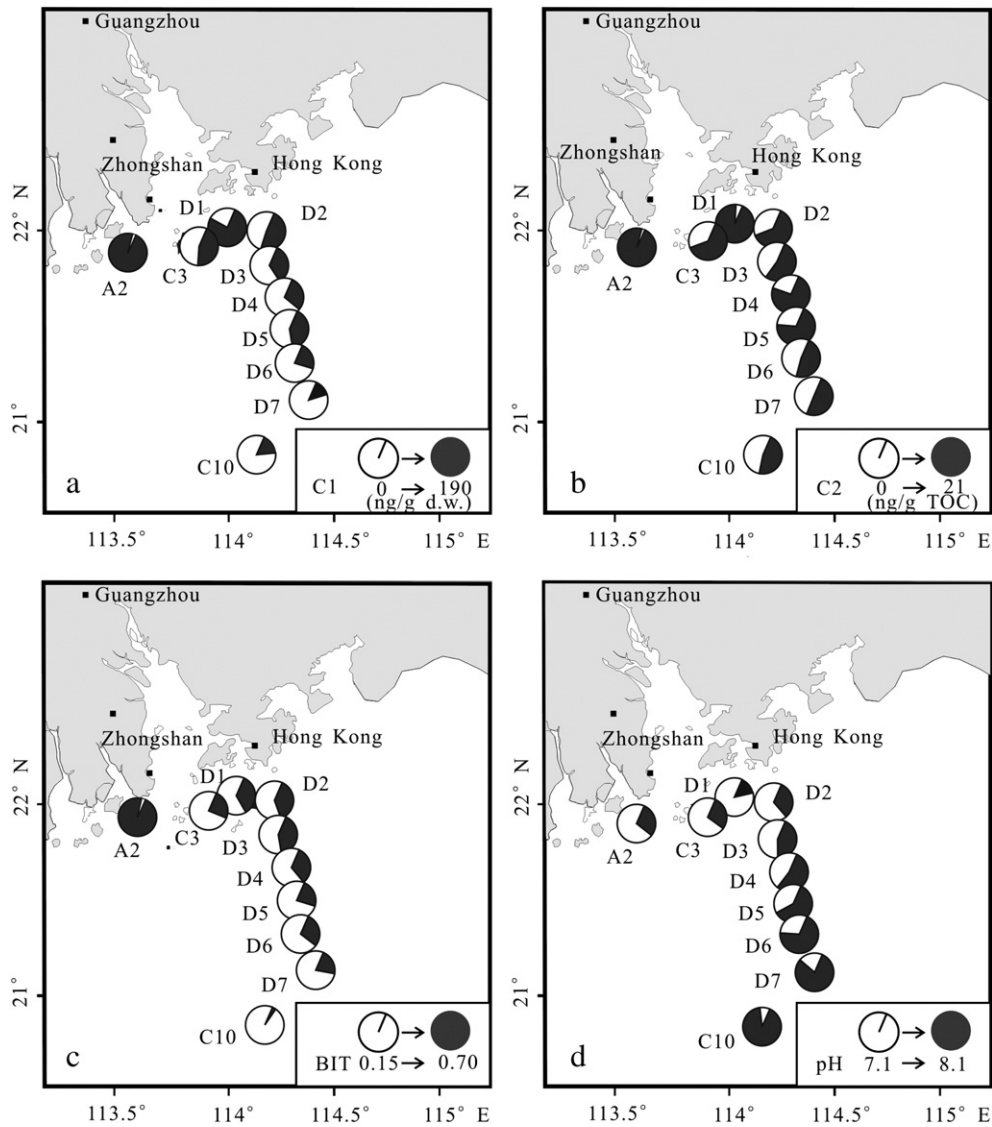
Fig. 2. Concentrations of branched glycerol dialkyl glycerol tetraethers (brGDGTs) normalized to (a) dry weight and (b) total organic carbon (TOC), and distributions of (c) the branched vs. isoprenoid tetraether (BIT) and (d) the cyclization ratio of branched tetraethers (CBT)-derived pH in the surface sediments from the Pearl River estuary.

using a high-performance liquid chromatography (HPLC)/atmospheric pressure positive ion chemical ionization mass spectrometry (APCI-MS) (Agilent 6410 QQQ LC–MS). The LC–MS was equipped with an auto-injection system and Agilent Chemstation software. Normal phase separation was achieved with a Prevail Cyano column (150 mm × 2.1 mm, 3 μm; Alltech, USA) maintained at 30 °C. The injection volume was 3 μL and the flow rate was 0.2 mL min^{-1}. The GDGTs were first eluted isocratically with a mixture of *n*-hexane (99%) and *n*-propanol (1%) for 5 min, followed by a linear gradient to 2% of *n*-propanol for 45 min. After each injection, the column was cleaned with a mixture of *n*-hexane (90%) and *n*-propanol (10%) for 15 min at 0.2 mL min^{-1}. The conditions for APCI-MS were as follows: nebulizer pressure 60 psi, vaporizer temperature 300 °C, drying gas (N$_2$) flow 5 L/min and temperature 200 °C, capillary voltage −2.5 kV, corona 5 μA. GDGTs were detected by selected ion monitoring (SIM) of the protonated molecules [M+H]$^+$ (dwell time 135 ms). Quantification was achieved by integration of the peak area of [M + H]$^+$ ion traces of GDGTs. The absolute amounts of GDGTs were calculated using an internal standard (C$_{46}$ GDGT) following Huguet et al. (2006). The average reproducibility of the indices, based on duplicate analysis of a selected number of sediment samples, is ±0.03 for the BIT index measurements and ±0.4 °C for the TEX$_{86}$ temperature estimates.

The equations used in this study are as follows:

$$BIT = \frac{[I] + [II] + [III]}{[I] + [II] + [III] + [Cren.]}.$$

TEX$_{86}^H$ and SST$_{86}^H$ were calculated following Kim et al. (2010):

$$TEX_{86}^H = \log\left(\frac{[GDGT-2] + [GDGT-3] + [Cren.']}{[GDGT-1] + [GDGT-2] + [GDGT-3] + [Cren.']}\right)$$

$$SST_{TEX86}^H = 68.4 \times TEX_{86}^H + 38.6.$$

The CBT and pH were calculated following Weijers et al. (2007):

$$CBT = -\log\left(\frac{[I_b + II_b]}{[Ia + IIa]}\right)$$

$$CBT = 3.33 - 0.38 \times pH.$$

3. Results

3.1. IsoGDGTs

IsoGDGTs and brGDGTs were detected in all sediment samples and their concentrations are given in Table 1. The concentrations of isoGDGTs were between 73.2 and 470.5 ng g^{-1} dry weight (dw), accounting for 64–94% of total GDGTs except for site A2 (43%, Table 1 and Fig. 2). These results suggest that the contribution of Archaea to the GDGT lipids in the studied sediments was larger than that of bacteria. The highest (lowest) abundances of isoGDGTs were found in the SCS (PRE) respectively (Table 1). The isoGDGTs were dominated by thaumarchaeol (cren.) and GDGT-0, accounting for 39–49% and 14–38% of total isoGDGTs, respectively. The compositional distributions of isoGDGTs exhibited different patterns in different areas. The highest GDGT-0 concentration was found in the YS and the lowest in the ECS. The GDGT-0/cren. ratios were between 0.3 and 1.0, and were higher in the YS (average: 0.8) than in the other study areas (average: 0.4).

3.2. BrGDGTs

The concentrations of brGDGTs (Table 1) were between 17.4 and 185.7 ng g^{-1} dw, accounting for 6–36% of total GDGTs, except for that in sample A2 (57%, Table 1). The highest brGDGT concentrations were found in the PRE (Table 1), followed by the YS and the ECS, with the lowest brGDGT concentrations in the SCS. In the PRE, the absolute concentrations of brGDGTs show an overall trend of progressive decrease away from the shore. However, this trend was not consistent for all sites, e.g., brGDGT concentration at site D5 was higher than that at site D4. This inconsistency in the trend was more obvious when the concentrations of brGDGTs were normalized to total organic carbon (TOC) contents (Fig. 2a and b).

The brGDGTs were dominated by those classed as GDGT-I (containing GDGT-Ia, Ib, and Ic, accounting for 31–60% of brGDGTs) and GDGT-II (33–41% of brGDGTs). The concentrations of those classified as GDGT-III, especially GDGT-IIIb and IIIc, occurred at low concentrations or even below detection limits. The brGDGTs without cyclopentane moieties (GDGT-Ia, IIa, and IIIa) were more abundant than their counterparts containing one or two cyclopentyl moieties in most of the sediments, except for some samples in the YS. Furthermore, the relative abundances of brGDGTs containing one cyclopentyl moiety (GDGT-Ib and IIb) were higher than those without cyclopentyl moieties (GDGT-Ia and IIa; e.g., YS-1, YS-4, and YS-5).

3.3. BIT and CBT values

Overall the values of the branched/isoprenoid index (BIT) index ranged from 0.09 to 0.42 (except A2, with BIT 0.68), and the mean values in the YS, ECS, and SCS were 0.23, 0.16, and 0.12, respectively (Table 1). The highest BIT value was found in the PRE. As a whole, the distribution of BIT values from the Pearl River mouth to the shelf of the SCS displayed a notable trend (Fig. 2c); the samples taken close to the coast had the highest BIT values (e.g., A2) (Table 1). In the inner shelf, BIT values generally decreased progressively seaward. However, the seaward decreasing trend in BIT values was not consistent e.g., the BIT value for D6 was higher than that of D5, and the value for D3 was higher than that of D2 (Fig. 2c).

The cyclisation ratio of branched tetraethers (CBT) values ranged from −0.15 to 0.58. The CBT-based pH values (Weijers et al., 2007) in the YS, ECS, SCS, and PRE were 8.3–9.2, 7.8–8.4, 7.7–8.1, and 7.2–8.0, respectively (Table 1). Notably, the CBT-derived pH values progressively increased seaward from the river mouth to the inner shelf and reached 8.0 at site C10 in the PRE (Fig. 2d).

3.4. TEX$_{86}^{H}$-derived temperatures

According to Kim et al. (2010), the thaumarchaeol region-isomer plays a more important role for temperature adaptation in (sub)tropical oceans than in (sub)polar oceans. In our study, the thaumarchaeol region-isomer content was similar to that of GDGTs 1–3 (Table 1), and we found that most of the mean annual SST in the study areas as determined by satellite remote sensing was above 15 °C. Therefore, the following discussion focuses on TEX$_{86}^{H}$ derived temperatures.

The TEX$_{86}^{H}$-derived temperatures (Kim et al., 2010, SST$_{86}^{H}$) were 15.2–27.2 °C in the study areas (Table 1). From north to south, the average SSTH 86 values were 17.1, 22.8, 22.6 and 26.1 °C in the YS, ECS, PRE and SCS, respectively. In comparison, the average of satellite-derived annual temperatures (SST$_{satellite}$, according to the NOAA global SST dataset) in the YS, ECS, PRE and SCS were 14.9, 22.1, 25.6 and 26.5 °C, respectively.

4. Discussion

4.1. Sources of brGDGTs in the studied areas and implications on pH

BrGDGTs have generally been attributed to soil bacteria (Sinninghe Damsté et al., 2000; Weijers et al., 2006b), possibly Acidobacteria (Sinninghe Damsté et al., 2011), which occur ubiquitously in soils, peats, lakes, and marine sediments (Sinninghe Damsté et al., 2000; Weijers et al., 2006b; Sinninghe Damsté et al., 2009; Tierney et al., 2010). For coastal marine sediments, brGDGTs were initially thought to be deposited after being transported by rivers from terrestrial soils; therefore, the BIT index, based on brGDGTs derived from anaerobic bacteria thriving in terrestrial environments (Weijers et al., 2006a) and thaumarchaeol predominantly produced by marine planktonic Thaumarchaeota (Sinninghe Damsté et al., 2002), was proposed as a proxy for the input of soil OM to aquatic environments (Hopmans and Weijers, 2004; Weijers et al., 2007). However, recent studies also suggested the in situ production of brGDGTs in anoxic parts of the water column and/or sediments of restricted fjords (Peterse et al., 2009) or sediments in lakes (Sinninghe Damsté et al., 2009).

The present study showed a pronounced spatial variability in the concentration of brGDGTs in coastal areas: the highest brGDGT concentrations (absolute values and relative to TOC) were found in the PRE where the spatial distribution of brGDGTs showed an inconsistent but overall seaward decreasing trend (Fig. 2a and b), which clearly did not reflect the Pearl River catchment soil conditions. This pattern was different from that described previously by Kim et al. (2006) and Walsh et al. (2008) for recent sediments in the NW Mediterranean (Gulf of Lyons) and Vancouver Island fjords. Furthermore, the values of the CBT index (the relative amount of cyclopentyl moieties), decreased seaward and the CBT-derived pH values increased seaward in the same way as the measured pH values (Chen et al., 2004), indicating that CBT-derived pH values was influenced by that of the ambient water pH. This implies that *in situ* production of brGDGTs was significant enough to overprint the signal of soil-derived brGDGT input. These characteristics of the brGDGT distribution reflect a mixture of sources, terrestrial soils in the river catchment and in situ production in the estuary. Previous studies also indicated aquatic production of brGDGTs in estuarine and coastal areas (Peterse et al., 2009; Zhu et al., 2011). Thus, in this case, the BIT index should not be applied directly to determine the relative contribution of terrestrial soil GDGTs to continental margins (Zhu et al., 2011). Detailed investigations are needed for the identification of aquatic sources and quantification of the production of brGDGTs found in marine sediments.

The concentration of brGDGTs and relative brGDGT proportions of the total GDGTs, being similar to BIT values, were higher in the YS than those in the ECS and SCS (Table 1), indicating more terrestrial soil input in the YS. The CBT-derived pH values in the YS were 8.3–9.2, which were higher than the pH values of normal marine water (8.1).
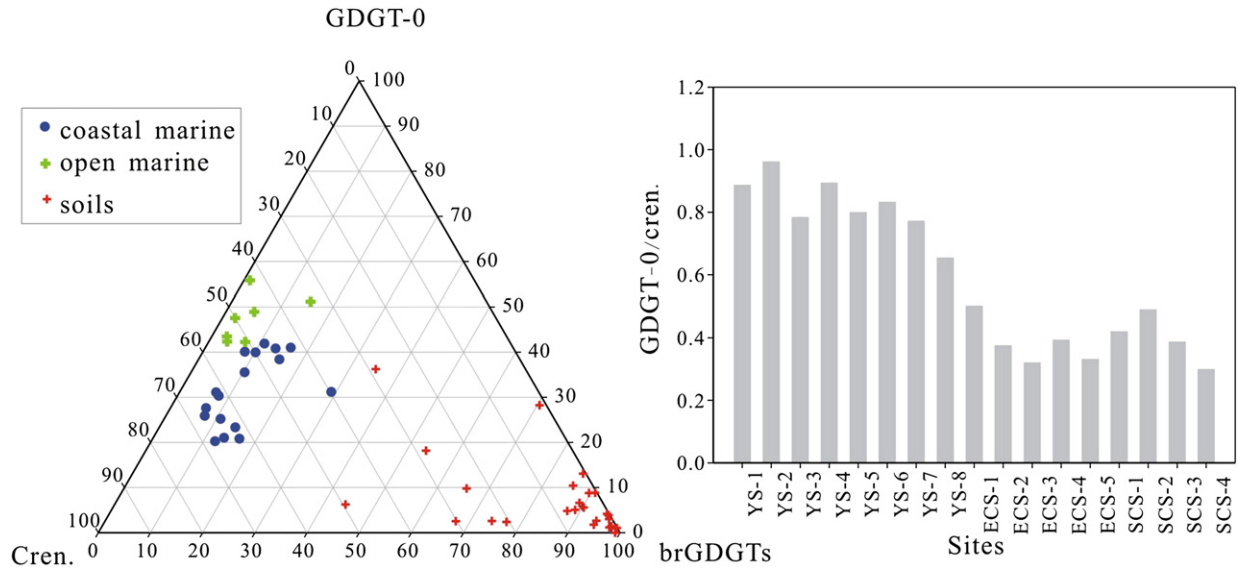
Fig. 3. (a) Ternary diagram showing the composition of the major GDGTs in the soils (data from Weijers et al., 2006b), open marine sediments as reported by Schouten et al. (2000) and coastal marine sediments in China Sea and (b) GDGT-0/cren. ratios in China Sea.

The range was similar to the pH values of basic soils in the lower Yellow River basin (7.5–9.0) (Xiong, 1986). There the abundances of Ib were higher than those of Ia in the YS sediments, similar to the distribution of brGDGTs in the Bohai Bay Basin, the lower Yellow River basin (calculated pH ranged from 7.5 to 9.0 based on CBT in soils). The results indicate that the brGDGTs in the sediments taken from the YS were mainly derived from soils transported by the Yellow River from its lower basin into the Yellow Sea.

The concentrations of brGDGT were lower in the ECS and SCS than those in the YS (Table 1). The CBT-derived pH values were 7.7–8.1, except for site ECS-1 (pH = 8.4) (Table 1). The CBT-derived pH values were higher than those of soils in the lower Yangtze River basin and terrestrial areas of South China (5.5–7.5, Xiong, 1986), indicating that the brGDGTs in the sediments of the coastal areas of the ECS and SCS also recorded the input contribution from marine sources. These results suggest that part of the brGDGTs in the coastal areas of the ECS and SCS might be produced in situ. Although a previous study (Yang et al., 2008) indicated that terrestrial OM (mainly derived from soils) can account for 5–57% of the total organic carbon in the Changjiang River Estuary and the ECS as determined by $\delta^{13}C$, C/N ratio and lignin content, the concentration of brGDGTs was relatively low in the ECS. The most likely explanation is that most of the soil-derived brGDGTs were degraded in the estuary (Zhu et al., 2011). While for the SCS, the low concentration of brGDGTs was likely due to low input of terrestrial OM (Wang et al., 2009), where the BIT values were relatively low (Table 1).

4.2. Sources of GDGT-0

A ternary diagram, illustrating the composition of the major GDGTs in the soil, peat, coastal and open marine environments (Fig. 3a). indicates greater contributions of cren. and GDGT-0 in marine settings than in terrestrial environments. The proportions of brGDGTs, GDGT-0 and cren. were 25:3:4 and the average ratio of GDGT-0/brGDGTs was 0.1 in the global terrestrial setting (Weijers et al., 2006b). In our study, the proportions of brGDGTs, GDGT-0, and cren. were 25:72:133 and the average ratio of GDGT-0/brGDGTs was 2.9; significantly higher than that calculated as an average for the global terrestrial environment. Therefore, the dominant source of GDGT-0 may be marine instead of terrestrial inputs. When the terrestrial portion of the inputs was deducted, assuming that all of the brGDGTs were derived from terrestrial sources, the average of GDGT-0/cren. was calculated to be between 0.3 and 1.0 in the coastal areas of China (Fig. 3b). It was shown that

the GDGT-0/cren. values were higher in the YS than in other study areas. GDGT-0 occurred not only in planktonic nonthermophilic Thaumarchaeota, but also in methanogenic Archaea that did not produce any GDGTs with cyclopentane rings. Therefore it is suggested that the relatively higher values of GDGT-0/cren. ratio in the YS may be of a methanogenic Archaea source, whose optimal growth temperature is mostly below 20 °C (Franzmann et al., 1992; von Klein et al., 2002), and are therefore likely to be thriving in the YS.

4.3. TEX_{86}^H temperatures

For most of the areas studied the mean annual SST was above 15 °C as determined by satellite remote sensing (Table 1), therefore, the TEX_{86}^H was chosen for the calculation of SST (Kim et al., 2010). The reconstructed SST_{86}^H ranged from 15.2 to 27.2 °C in the studied areas (Table 1). Comparison of these temperatures with satellite-derived temperatures shows a positive correlation between SST_{86}^H and $SST_{satellite}$ (Fig. 4, $R^2 = 0.78$, for samples having BIT < 0.3). Therefore,
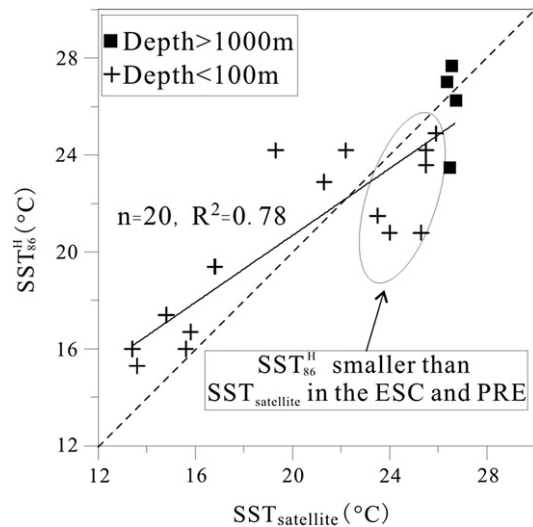

Fig. 4. Relationship between the tetraether index of tetraethers consisting of 86 carbon atoms (TEX_{86}^H)-derived and satellite-derived sea surface temperature (SST_{86}^H and $SST_{satellite}$, pluses (+) and squares (■) show site water depth <100 m and >1000 m, respectively).

the results of the present study suggest that the TEX_{86}^H proxy could be applicable to the reconstruction of SST in the studied areas and, potentially, in similar settings.

The depth of sampling stations in the SCS are >1000 m, and all the other areas are <100 m. Therefore the factors that influence the distributions of GDGTs might be significantly different, e.g. seasonal effects on blooms of tetraether-producing Thaumarchaeota (Zhang et al., 2013). Therefore, these areas that have different bathymetric settings are discussed separately below.

In the shallow areas, the correlation between SST_{86}^H and annual $SST_{satellite}$ ($R^2 = 0.78$, for samples having BIT < 0.3) was slightly lower than that for TEX_{86}^H-SST from global regression (Kim et al., 2010, $R^2 = 0.87$). One interpretation for this phenomenon could be attributed to the interference from GDGTs derived from terrestrial sources, which had a significant impact, as large differences in the distributions of land and water column derived GDGTs could cause a bias at relatively low BIT index values (<0.3). Based on the currently limited dataset, the calculated temperatures in the YS and northern ECS were higher than the annual $SST_{satellite}$, while the opposite relation was observed in the PRE and southern ECS. These results suggest that in tropical region, the TEX_{86} temperature estimates are lower in samples with higher BIT values, while the opposite holds for cold regions.

Another explanation is that GDGTs in nearshore sediments were influenced by seasonality. The relatively better correlation between SST_{86}^H and summer SST-$_{satellite}$ ($R^2 = 0.84$, for samples having BIT < 0.3) in the YS and northern ECS suggests that SST_{86}^H might be biased towards warmer season temperatures if the source organisms thrive in those periods. Recent evidence suggests that some Thaumarchaeota were nitrifiers (Wuchter et al., 2006) and use ammonia, in the manner that phytoplankton and zooplankton do, as an energy source at a competitive disadvantage (Murray et al., 1999). In the YS and northern ECS, the presence of large phytoplankton blooms observed in spring, which may outcompete the marine Thaumarchaeota (Wuchter et al., 2006). By contrast, phytoplankton productivity was greatly reduced during summer which could have led to a significant increase in ammonia availability and thus induced higher *Taumarchaeota* productivity (Sinninghe Damsté et al., 2009). In this case, the SST_{86}^H was likely to imprint the information of summer SST in these areas, which is consistent with previous observations showing that surface water *Taumarchaeota* populations were abundant during warm season in temperate areas (e.g. Alonso-Sáez et al., 2008; Leider et al., 2010).

However, this is not the case in the subtropical-tropical southern ECS and PRE, where the TEX_{86}^H-derived temperatures were overall lower than the annual $SST_{satellite}$ values (for samples with BIT < 0.3), reflecting the winter SST. The lower than expected TEX_{86}^H temperatures in these areas might be attributed to the bloom of *Taumarchaeota* in winter. The phytoplankton production declines in winter due to decreased terrestrial nutrient influx, and lower water column light caused by higher load of suspended particles (Tang et al., 2007). Moreover, the calculated temperatures substantially decrease shoreward, in agreement with the winter SST distribution when nutrient and algal production declines. For sites located in the Taiwan Straits (e.g. ECS-4 and ECS-5) and in the PRE (e.g. C10 and D7), the values of calculated SST_{86}^H were significantly lower than those of most seasonal and average $SST_{satellite}$ (Table 1). This might be due to the influence of China's coastal current (Li and You, 2003), especially, in the Taiwan Straits the current flows along the coast of Mainland China, moving from north to south (Lin et al., 2005), which transported the GDGTs produced in northern colder sea areas into the southern region.

In the SCS, the sampling sites are located at water depths of >1000 m, the SST_{86}^H values (except SCS-4) matched well with the $SST_{satellite}$ ones (Table 1), similar to the results inferred from the coretop sediments by Wei et al. (2011), suggesting that the TEX_{86} proxy could be used universally to calculate the SST in the SCS with water depth >1000 m. However, Jia et al. (2012) found that TEX_{86}^H correlated better with the annual mean temperature in the subsurface water

column (30–125 m) than that in surface waters (0–30 m) in the SCS. In our study, the correlation between SST_{86}^H and annual mean temperature in subsurface water is not better than that with temperature in surface water at these four sites. Therefore, for the limited dataset, TEX_{86}^H-based temperatures for surface sediments of deep water sites (depths >1000 m) generally reflected the satellite mean annual sea surface temperatures in the SCS.

5. Summary and conclusions

The study of GDGTs from surface sediments taken at depths of either <100 m or >1000 m along transects in various oceanographic settings in the sea around China revealed that:

1) The distribution of GDGTs reflect their biological sources and their respective habitats. A striking example was that the distributions of brGDGTs in the YS were similar to those in the lower Yellow River basin, indicating that these brGDGTs were primarily of terrestrial-soil origin. However, the variability of CBT-derived pH values in the PRE suggest that branched GDGTs might also be produced in situ in the sediment or water column.

2) TEX_{86}^H-derived temperatures are better correlated to satellite-based temperatures for samples with BIT values <0.3, although the regression ($R^2 = 0.78$, n = 20) was slightly weaker than for the global calibration dataset. In the shallow areas (water depth <100 m), a systematic difference between SST_{86}^H and $SST_{satellite}$ in the coastal areas of China might point to the effect of GDGTs derived from terrestrial inputs or seasonal bloom of *Thaumarchaeota* in different oceanographic settings.

3) A large difference between warmer $SST_{satellite}$ and colder SST_{86}^H in sediments was found in the Taiwan Straits (e.g. ECS-4 and ECS-5) and south of Guangdong (e.g. C3 and D3). This may point to the effect of the north to south long shore current in transporting the biological proxies from the source area into the sediments in a different oceanographic setting.

Appendix A. Supplementary data

Supplementary data associated with this article can be found in the online version, at http://dx.doi.org/10.1016/j.palaeo.2013.12.006. These data include Google map of the most important areas described in this article.

References

Alonso-Sáez, L., Sánchez, O., Gasol, J.M., Balagué, V., Pedrós-Alio, C., 2008. Winter-to-summer changes in the composition and single-cell activity of near-surface Arctic prokaryotes. Environ. Microbiol. 10, 2444–2454.

Brassell, S.C., Eglinton, G., Marlowe, I.T., Pflaumann, U., Sarnthein, M., 1986. Molecular stratigraphy: a new tool for climatic assessment. Nature 320, 129–133.

Brochier-Armanet, C., Boussau, B., Gribaldo, S., Forterre, P., 2008. Mesophilic Crenarchaeota: proposal for a third archaeal phylum, the Thaumarchaeota. Nat. Rev. Microbiol. 6, 245–252.

Chen, J.F., Yan, L., Yin, K.D., Jin, H.Y., 2004. Amino acids in the Pearl River Estuary and adjacent waters: origins, transformation and degradation. Cont. Shelf Res. 24, 1877–1894.

De La Torre, J.R., Walker, C.B., Ingalls, A.E., Könneke, M., Stahl, D.A., 2008. Cultivation of a thermophilic ammonia oxidizing archaeon synthesizing crenarchaeol. Environ. Microbiol. 10, 810–818.

De Rosa, M., Gambacorta, A., 1988. The lipids of archaebacteria. Prog. Lipid Res. 27, 153.

Franzmann, P.D., Springer, N., Ludwig, W., Demacario, E.C., Rohde, M., 1992. A methanogenic archaeon from ace lake, Antarctica. Syst. Appl. Microbiol. 15, 573–581.

Ge, H.M., Zhang, C.L., Dang, H.Y., Zhu, C., Jia, G.D., 2013. Distribution of tetraether lipids in surface sediments of the northern South China Sea: implications for TEX$_{86}$ proxies. Geosci. Front. 4, 223–229.

Hopmans, E.C., Weijers, J.W.H., 2004. A novel proxy for terrestrial organic matter in sediments based on branched and isoprenoid tetraether lipids. Earth Planet. Sci. Lett. 224, 107–116.

Hu, J.F., Meyers, P.A., Chen, G.K., Peng, P.A., Yang, Q.H., 2012. Archaeal and bacterial glycerol dialkyl glycerol tetraethers in sediments from the Eastern Lau Speading Center, South Pacific Ocean. Org. Geochem. 43, 162–167.

Huguet, C., Hopmans, E.C., Febo-Ayala, W., Thompson, D.H., Sinninghe Damsté, J.S., Schouten, S., 2006. An improved method to determine the absolute abundance of glycerol dibiphytanyl glycerol tetraether lipids. Org. Geochem. 37, 1036–1041.

IPCC: Climate Change, 2007. The Physical Science Basis — Contribution of Working Group I to the Fourth Assessment Report of the Intergovernmental Panel on Climate Change. In: Solomon, S., Qin, D., Manning, M., Marquis, M., Averyt, K., Tignor, M.M.B., LeRoy Miller, H.J. (Eds.), Cambridge University Press.

Jia, G.D., Zhang, J., Chen, J.F., Peng, P.A., Zhang, C.L., 2012. Archaeal tetraether lipids record subsurface water temperature in the South China Sea. Org. Geochem. 50, 68–77.

Kim, J.H., Schouten, S., Buscail, R., Ludwig, W., Bonnin, J., Sinninghe Damsté, J.S., Bourrin, F., 2006. Origin and distribution of terrestrial organic matter in the NW Mediterranean (Gulf of Lions): exploring the newly developed BIT index. Geochem. Geophys. Geosyst. 7, Q11017.

Kim, J.H., Schouten, S., Hopmans, E.C., Donner, B., Sinninghe Damsté, J.S., 2008. Global sediment core-top calibration of the TEX$_{86}$ paleothermometer in the ocean. Geochim. Cosmochim. Acta 72, 1154–1173.

Kim, J.H., van der Meer, J., Schouten, S., Helmke, P., Willmott, V., Sangiorgi, F., Koc, N., Hopmans, E.C., Sinninghe Damsté, J.S., 2010. New indices and calibrations derived from the distribution of crenarchaeal isoprenoid tetraether lipids: implications for past sea surface temperature reconstructions. Geochim. Cosmochim. Acta 74, 4639–4654.

Leider, A., Hinrichs, K.-U., Mollenhauer, G., Versteegh, G.J.M., 2010. Core-top calibration of the lipid-based UK 37 and TEX$_{86}$ temperature proxies on the southern Italian shelf (SW Adriatic Sea, Gulf of Taranto). Earth Planet. Sci. Lett. 300, 112–124.

Li, R.F., You, X.B., 2003. The development and application of the oceanic general circulation models part II. The regional oceanic general circulation models. Chin. J. Atmos. Sci. 27 (4), 729–739.

Li, D., Zhao, M., Tian, J., Li, L., 2013. Comparison and implication of TEX$_{86}$ and U$^{K}_{37}$ temperature records over the last 356 kyr of ODP Site 1147 from the northern South China Sea. Palaeogeogr. Palaeoclimatol. Palaeoecol. 376, 213–223.

Lin, S.F., Tang, T.Y., Jan, S., Chen, C.J., 2005. Taiwan Strait current in winter. Cont. Shelf Res. 25, 1023–1042.

Murray, A.E., Blakis, A., Massana, R., Strawzewski, S., Passow, U., Alldredge, A., DeLong, E.F., 1999. A time series assessment of planktonic archaeal variability in the Santa Barbara Channel. Aquat. Microb. Ecol. 20, 129–145.

Pearson, A., Huang, Z., Ingalls, A.E., Romanek, C.S., Wiegel, J., Freeman, K.H., Smittenberg, R.H., Zhang, C.L., 2004. Nonmarine crenarchaeol in Nevada hot springs. Appl. Environ. Microbiol. 70, 5229–5237.

Peterse, F., Kim, J.H., Schouten, S., Kristensen, D.K., Sinninghe Damsté, J.S., 2009. Constraints on the application of the MBT/CBT palaeothermometer at high latitude environments (Svalbard, Norway). Org. Geochem. 40, 692–699.

Pitcher, A., Schouten, S., Sinninghe Damsté, J.S., 2009. In situ production of Crenarchaeol in two California hot springs. Appl. Environ. Microbiol. 75, 4443–4451.

Powers, L.A., Werne, J.P., Johnson, T.C., Hopmans, E.C., Sinninghe Damsté, J.S., Schouten, S., 2004. Crenarchaeotal membrane lipids in lake sediments: a new paleotemperature proxy for continental paleoclimate reconstruction? Geology 32, 613–616.

Powers, L, Werne, J.P., Vanderwoude, A.J., Sinninghe Damsté, J.S., Hopmans, E.C., Schouten, S., 2010. Applicability and calibration of the TEX$_{86}$ paleothermometer in lakes. Org. Geochem. 41, 404–413.

Schouten, S., Hopmans, E.C., Pancost, R.D., Sinninghe Damsté, J.S., 2000. Widespread occurrence of structurally diverse tetraether membrane lipids: evidence for the ubiquitous presence of low-temperature relatives of hyperthermophiles. PNAS 97, 14421–14426.

Schouten, S., Hopmans, E.C., Schefuss, E., Sinninghe Damsté, J.S., 2002. Distributional variations in marine Crenarchaeotal membrane lipids: a new tool for reconstructing ancient sea water temperatures? Earth Planet. Sci. Lett. 204, 265–274.

Schouten, S., van der Meer, M.T.J., Hopmans, E.C., Rijpstra, W.I., Reysenbach, A.-L, Ward, D.M., Sinninghe Damsté, J.S., 2007. Archaeal and bacterial glycerol dialkyl glycerol tetraether lipids in hot springs of Yellowstone national park. Appl. Environ. Microbiol. 73, 6181–6191.

Shintani, T., Yamamoto, M., Chen, M.-T., 2011. Paleoenvironmental changes in the northern South China Sea over the past 28,000 years: a study of TEX$_{86}$-derived sea surface temperatures and terrestrial biomarkers. J. Asian Earth Sci. 40, 1221–1229.

Sinninghe Damsté, J.S., Hopmans, E.C., Pancost, R.D., Schouten, S., Geenevasen, J.A.J., 2000. Newly discovered non-isoprenoid glycerol dialkyl glycerol tetraether lipids in sediments. Chem. Commun. 1683–1684.

Sinninghe Damsté, J.S., Rijpstra, W.I.C., Hopmans, E.C., Prahl, F.G., Wakeham, S.G., Schouten, S., 2002. Distribution of membrane lipids of planktonic Crenarchaeota in the Arabian Sea. Appl. Environ. Microbiol. 68, 2997.

Sinninghe Damsté, J.S., Ossebaar, J., Abbas, B., Schouten, S., Verschuren, D., 2009. Fluxes and distribution of tetraether lipids in an equatorial African lake: constraints on the application of the TEX$_{86}$ palaeothermometer and BIT index in lacustrine settings. Geochim. Cosmochim. Acta 73, 4232–4249.

Sinninghe Damsté, J.S., Rijpstra, W.I.C., Hopmans, E.C., Weijers, J.W.H., Foesel, B.U., Overmann, J., Dedysh, S.N., 2011. 13,16-dimethyl Octacosanedioic acid (iso-diabolic acid), a common membrane-spanning lipid of acidobacteria subdivisions 1 and 3. Appl. Environ. Microbiol. 77, 4147–4154.

Spang, A., Hatzenpichler, R., Brochier-Armanet, C., Rattei, T., Tischler, P., Spieck, E., Streit, W., Stahl, D.A., Wagner, M., Schleper, C., 2010. Distinct gene set in two different lineages of ammonia-oxidizing Archaea supports the phylum Thaumarchaeota. Trends Microbiol. 18, 331–340.

Tang, S.L., Chen, C.Q., Zhan, H.G., Xu, D.Z., Liu, D.Z., 2007. Retrieval of euphotic layer depth of South China Sea by remote sensing. J. Trop. Oceanogr. 26, 9–15.

Tierney, J.E., Russell, J.M., Eggermont, H., Hopmans, E.C., Verschuren, D., Sinninghe Damsté, J.S., 2010. Environmental controls on branched tetraether lipid distributions in tropical East African lake sediments. Geochim. Cosmochim. Acta 74, 4902–4918.

von Klein, D., Arab, H., Volker, H., Thomm, M., 2002. *Methanosarcina baltica*, sp. nov., a novel methanogen isolated from the Gotland Deep of the Baltic Sea. Extremophiles 6, 103–110.

Walsh, E.M., Ingalls, A.E., Keil, R.G., 2008. Sources and transport of terrestrial organic matter in Vancouver Island Fjords and the Vancouver-Washington margin: a multiproxy approach using δ^{13}C org, lignin phenols, and the ether lipid BIT Index. Limnol. Oceanogr. 53, 1054–1063.

Wang, L.L., Hu, J.F., Tang, J.H., 2009. Amino acid composition and its biogeochemistry implications of surface sediments in coastal areas of China. Acta Oceanol. Sin. 31, 161–169 (in Chinese, with English abstract).

Wei, Y.L., Wang, J.X., Liu, J., Dong, L., Li, L., Wang, H., et al., 2011. Spatial variations in archaeal lipids of surface water and core-top sediments in the South China Sea and their implications for paleoclimate studies. Appl. Environ. Microbiol. 77, 7479–7489.

Weijers, J.W.H., Schouten, S., Hopmans, E.C., Geenevasen, J.A.J., David, O.R.P., Coleman, J.M., Pancost, R.D., Sinninghe Damsté, J.S., 2006a. Membrane lipids of mesophilic anaerobic bacteria thriving in peats have typical archaeal traits. Environ. Microbiol. 8, 648–657.

Weijers, J.W.H., Schouten, S., Spaargaren, O.C., Sinninghe Damsté, J.S., 2006b. Occurrence and distribution of tetraether membrane lipids in soils: implications for the use of the TEX$_{86}$ proxy and the BIT index. Org. Geochem. 37, 1680–1693.

Weijers, J.W.H., Schouten, S., Van den Donker, J.C., Hopmans, E.C., Sinninghe Damsté, J.S., 2007. Environmental controls on bacterial tetraether membrane lipid distribution in soils. Geochim. Cosmochim. Acta 71, 703–713.

Wuchter, C., Schouten, S., Coolen, M.J.L., Sinninghe Damsté, J.S., 2004. Temperature-dependent variation in the distribution of tetraether membrane lipids of marine Crenarchaeota: implications for TEX$_{86}$ paleothermometry. Paleoceanography 19, PA4028.

Wuchter, C., Schouten, S., Wakeham, S.G., Sinninghe Damsté, J.S., 2005. Temporal and spatial variation in tetraether membrane lipids of marine Crenarchaeota in particulate organic matter: implications for TEX$_{86}$ paleothermometry. Paleoceanography 20, 1–11.

Wuchter, C., Herfort, L., Coolen, M.J.L., Abbas, B., Timmers, P., Strous, M., Herndl, G.J., Middelburg, J.J., Schouten, S., Sinninghe Damsté, J.S., 2006. Archaeal nitrification in the ocean. Proc. Natl. Acad. Sci. U. S. A. 103, 12,317–12,322.

Xiong, Y., 1986. Soil Atlases of China. Cartographic Pressing House, Beijing 33–34 (in Chinese).

Yang, L., Wu, Y., Zhang, J., Yu, H., Zhang, G., Zhu, Z., 2008. Distribution of lignin and sources of organic matter in surface sediments from the adjacent area of the Changjiang Estuary in China. Acta Oceanol. Sin. 30 (5), 35–42 (in Chinese, with English abstract).

Ying, Z.F., 1994. The frontal classification and its influence on sedimentation in Lingdingyang of Pearl River estuary. Trop. Oceanol. 13, 25–31 (in Chinese, with English abstract).

Zhang, C.L., Pearson, A., Li, Y.L., Mills, G., Wiegel, J., 2006. Thermophilic temperature optimum for crenarchaeol synthesis and its implication for archaeal evolution. Appl. Environ. Microbiol. 72, 4419–4422.

Zhang, J., Bai, Y., Xu, S., Lei, X., Jia, G., 2013. Alkenone and tetraether lipids reflect different seasonal seawater temperatures in the coastal northern South China Sea. Org. Geochem. 58, 115–120.

Zhu, C., Weijers, J.W.H., Wagner, T., Pan, J.M., Chen, J.F., 2011. Sources and distributions of tetraether lipids in surface sediments across a large river-dominated continental margin. Org. Geochem. 42 (4), 376–386.